EFDA-JET-CP(06)05-14

S.E. Sharapov, B. Alper, Yu.F. Baranov, H.L. Berk, D. Borba, C. Boswell,
B.N. Breizman, C.D. Challis, M.de Baar, P.de Vries, S. Hacquin, N.C.Hawkes,
V.G. Kiptily, H.R. Koslowski, J. Mailloux, M. Nave, S.D. Pinches,
P. Sandquist, N.P. Young and JET EFDA contributors

Development of Alfvén Spectroscopy in Advanced Scenarios on JET

Development of Alfvén Spectroscopy in Advanced Scenarios on JET

S.E. Sharapov[1], B. Alper[1], Yu.F. Baranov[1], H.L. Berk[2], D. Borba[3], C. Boswell[4], B.N. Breizman[2], C.D. Challis[1], M.de Baar[5], P.de Vries[1], S. Hacquin[3], N.C.Hawkes[1], V.G. Kiptily[1], H.R. Koslowski[6], J. Mailloux[1], M. Nave[3], S.D. Pinches[1], P. Sandquis[7]t, N.P. Young[8] and JET EFDA contributors*

[1]Euratom/UKAEA Fusion Association, Culham Science Centre, Abingdon, OX14 3DB, UK.
[2]IFS, University of Texas at Austin, Austin, USA
[3]Euratom/IST Fusion Association, Centro de Fusao Nuclear, Lisboa, Portugal
[4]PSFC, Massachussets Institite of Technology, Cambridge, USA
[5]Assoc. Euratom-FOM Institute Plasmaphys. 'Rijnhuizen', Nieuwegein, The Netherlands
[6]Forschungszentrum Jülich GmbH, Euratom Association, Jülich, Germany
[7]Euratom/VR Fusion Association, Chalmers University of Technology, Goteborg, Sweden
[8]Warwick University, Coventry, UK
** See annex of M. L. Watkins et al, "Overview of JET Results",*
(Proc. 21st IAEA Fusion Energy Conference, Chengdu, China (2006)).

Preprint of Paper to be submitted for publication in Proceedings of the
21st IAEA Fusion Energy Conference,
(Chengdu, China, 16th October - 22nd October 2006)

ABSTRACT.

Measurements of low-amplitude Alfvén Eigenmodes (AEs) excited by fast ions represent an attractive form of MHD spectroscopy of fusion plasmas, which can provide data on plasma equilibrium and plasma parameters. Techniques for detecting Alfvén Cascades (ACs) and Toroidal Alfvén Eigenmodes (TAEs) with the use of interferometry and X-mode reflectometry demonstrate on JET an attractive approach to such measurements, complementary and sometimes superior to the magnetic measurements with Mirnov coils. With the use of O-mode interferometry, allowing a very high time resolution for detecting ACs, the correlation between the Internal Transport Barrier (ITB) triggering events and low rational values of q_{min} (t) has been assessed in JET plasmas with non-monotonic q(r) -profiles. It was found that in the majority of cases where the ITB were triggered near integer q_{min} (t) in plasmas with non-monotonic q(r) -profiles, the ITB triggering event preceded a grand ACs. Since grand ACs mark the time of q_{min} (t) = integer, this observation indicates strongly that the ITB triggering event is associated with the depletion of rational magnetic surfaces just before q_{min} (t) = integer, rather than with the presence of an integer q_{min} (t) value itself. The correlation between ITB triggering events and grand ACs has been found to exist in JET plasmas with high densities, up to 5×10^{19} m^{-3}, showing that the timing of ITB triggering from AC diagnosis may facilitate scenario development in machines with high plasma densities such as C-MOD and ITER. ACs driven by sub-Alfvenic NBI were detected on JET using O-mode interferometry in JET experiments with Tritium NBI. Although considerable NBI-driven AC activity was present, a good agreement was found both in the radial profile and in the time evolution of DT neutrons between the neutron measurements and TRANSP code, indicating the ACs have at most a small effect on fast particle confinement in this case. Transitions from TAEs to ACs have been observed on JET when an ITB forms. It was found that the observed TAE-to-AC transition is caused by a reversal of the magnetic shear, mainly associated with the bootstrap current. ACs were also observed in high-temperature JET plasmas with monster sawteeth, and the use of Alfvén spectroscopy shows that the sawtooth crashes happen at $q_{min} \cong 0.85$, while $q_{min} > 1$ is deduced for the post-crash phase. The theory of ACs now includes thermal plasma effects and fast ion response, which enable determination of kinetic plasma parameters from AC measurements

1. INTRODUCTION

Alfvén Eigenmodes driven by energetic particles are routinely seen in JET plasmas heated by Ion Cyclotron Resonance Frequency (ICRF) waves and/or by Neutral Beam Injection (NBI). Measurements of such AEs with low amplitude represent an attractive form of MHD spectroscopy, called Alfvén spectroscopy, which solves the inverse problem of identifying plasma equilibrium and plasma parameters from the observed spectrum of the plasma perturbations [1–3]. AEs are attractive since they are robust and numerous in most of the machines with fast ions, and these modes do not cause significant degradation of plasma or the fast ion confinement as long as AE amplitudes are sufficiently small. The use of Alfvén spectroscopy has become routine for JET advanced scenarios, since the detection of ACs and TAEs helps to identify the existence of reversed magnetic shear and provide

accurate data on the evolution of q_{min} (t) [2], which is needed for developing scenarios with ITBs. Recent progress in Alfvén spectroscopy on JET has been developed along two main avenues: improving techniques of AE detection with the use of interferometry and reflectometry; and applying Alfvén spectroscopy to new phenomena over a broader range of plasma parameters.

2. DEVELOPMENT OF INTERFEROMETRY AND REFLECTOMETRY TECHNIQUES FOR DETECTING ALFVÉN EIGENMODES

It has long been recognised that measurements of plasma density fluctuations associated with AEs using *reflectometry* have a number of advantages when compared to the external Mirnov coils: they allow the detection of highly localised perturbations in the plasma core and may provide a spatial coverage of the detected perturbations [4]. An important new way of detecting plasma density perturbations associated with AEs with the use of *interferometry* has been demonstrated more recently [5]. In this approach [5], an O-mode reflectometry system was used on JET with the microwave probing frequency above the cut-off frequency of the plasma. The interferometry measurements of plasma density perturbations associated with ACs showed an unprecedented frequency and time resolution, superior to that obtained with external magnetic coils. Reflectometry and interferometry measurements similar to that described in [4, 5] are now anticipated to play a yet larger role in detecting AEs in the harsh burning plasma environment of ITER, where the use of Mirnov coils may be problematic. In order to further assess and improve the interferometry/reflectometry techniques, three important steps have been made on JET: **1)** A complete description of the microwave beam propagation has been performed in 1D and 2D and a technique for calculating the amplitude of the electron density perturbations has been developed and validated against JET data [6]. 2) The standard JET interferometer with vertical lines-of-sight operating in the far infra-red range has also been shown to detect AEs [7], and **3)** The X-mode reflectometry system on JET has been improved and was also shown to perform well in detecting AEs [8].

2.1 O-MODE INTERFEROMETRY ON JET

It was found on JET [5] that the best way of detecting density fluctuations in the core region from O-mode reflectometry is to use a probing frequency above the cut-off frequency along the line of sight. In this case the refractive index for the O-mode wave,

$$N_O(f, R) = [1 - n_e(R) / n_c(f)]^{1/2} \tag{1}$$

remains positive all along the line of sight so that the probing wave propagates without being reflected by the plasma. The critical density n_c in Eq.(1) is proportional to the square of the probing wave frequency f:

$$n_c(f) = 4\pi^2 \varepsilon_0 m_e f^2 / e^2, \tag{2}$$

where e_o, m_e and e are the vacuum permittivity, the electron mass and the electron charge respectively. Launched from the outer side of the JET torus, R_e = 4m, as Figure 1 (bottom) shows, the probing microwave beam is reflected by the inner-wall at R_i = 2m, and then returns to the detector after a round trip along the probing line of sight in the whole plasma region. In this situation, the O-mode reflectometer acts as an interferometer and the whole plasma (including the core and high field side regions) is probed. The interferometry regime proves to be quite efficient for detecting ACs (see example in Figs.1,2) even in JET plasmas with high power NBI heating where ACs are not detected with external Mirnov coils [9].

The density perturbations associated with ACs cause strong perturbations of the received Omode beam signal, clearly observable in both its amplitude and its phase. The level of the AC density perturbations can be inferred from the phase shift $\varphi(f)$ of the probing wave after its double passage through the plasma in the geometric optics approximation as:

$$\varphi\,(f,\,t) = \frac{4\pi f}{c}\int_{R_e}^{R_i}\sqrt{1-\frac{n_e\,(R,\,t)}{n_e}}\;dR - \varphi_0 = \frac{4\pi f}{c}\int_{R_e}^{R_i}\sqrt{1-\frac{<n_0\,(R)> + \delta n_e\,(R,\,t)}{n_e}}\;dR - \varphi_0\,, \qquad (3)$$

provided that both the emitter and receiver are located at $R = R_e$. Here, $R = R_e$ is the inner wall position, $< n_0(R) >$ represents the equilibrium density profile and time-varying density fluctuations $\delta n_e\,(R,\,t)$ are caused by AEs. A full-wave computation using a 1D finitedifference code has been used for assessing the validity of the geometric optics approach above. Relative error in the phase estimate between the geometric optics and the full-wave phases of less than 1% was found for most JET experiments measuring ACs with typical frequency about 100kHz. The validity of the 1D approximation in (3) has been assessed then with the use of a full-wave 2D code. It was found that the relative difference in the phase obtained in the 1D approximation and in the 2D case is below 5% provided the poloidal width of an AC is larger than 5cm – a condition valid for poloidal mode numbers $m < 30$, i.e. for most JET cases. The use of the relation (3) shows that the typical level of the density perturbations associated with ACs is about $\delta n_e/n_e \geq 10^{-3}$ on the Low magnetic Field Side (LFS) of the torus, and this level is somewhat higher on the High Field Side (HFS) of the torus, in accordance with the ballooning character of the density perturbations in AC [5].

2.2 INFRA-RED INTERFEROMETRY OF AES ON JET

The standard JET interferometer with vertical lines-of-sight, shown in Figure 3, operates in the far infra-red range and is used on JET for density measurements. In order to assess the possibility to detect AEs with such an instrument, a high-frequency data acquisition system has been connected to this interferometer [7]. It was found that interferometry of this type also detects AEs and the signal quality is quite satisfactory as Figure 4 shows. The possibility of using this interferometry technique for the detection of AEs may be of importance for ITER in view of the problem with using Mirnov coils for detecting high-frequency AEs.

2.3 RENEWED LOW-NOISE X-MODE REFLECTOMETRY ON JET

The main limitation of using interferometry for detecting AEs, is that the AEs cannot be localised directly from the measurements. In the past, a cross-correlation between the interferometry data and other diagnostic data was explored on JET in order to overcome this limitation [2, 7]. A more direct approach can be achieved with the use of X-mode reflectometry [4]. Four new low-loss waveguides have been installed in JET for the X-mode reflectometer, affording the opportunity to carry out detailed correlation measurements on the localisation of AEs. Dedicated experiments were performed on JET scanning both the equilibrium magnetic field and plasma density, in which the performance and limitations of the renewed X-mode reflectometry were assessed. Figure 5 shows the evolution of cut-off layers for different fixed-frequency X-mode microwave beams, while Figure 6 shows the observed AEs, both ACs and TAEs, seen with one of the beams at 92GHz. The time slice of the phase perturbations from various channels confirms the expected localisation of the AC on both LFS, $R \cong 3.35m$, and HFS, $R \cong 2.55m$, regions. Due to the localisation region of the ACs associated with the zero shear magnetic surface at min q , determining the AC radial localisation provides information on the two-dimensional evolution of q_{min} (R, t) [8] required for developing a scenario with a wider ITB on JET.

3. TRIGGERING OF ITBS BY LOW-ORDER RATIONAL q_{MIN} AND ALFVÉN GRAND-CASCADES

One of the most intriguing problems in advanced tokamak scenarios is the correlation between the ITB triggering events and low rational values of q_{min} [10] in plasmas with nonmonotonic q (r) - profiles. The time sequence of ITB triggering events and q_{min} $(t) = integer$ surfaces appearing in the plasma during the current ramp-up phase of shear-reverse scenario, is of major interest. Using O-mode interferometry allows AC observation even when Mirnov coils detect no such signal, making it possible to identify the exact time of $q_{min} = integer$ events via *Alfvén grand cascades* (ACs with all mode numbers excited simultaneously [2]). Figure 2 shows a typical JET discharge with ICRF and NBI resulting in rapid toroidal rotation of the plasma, in which a grand cascade at $t \sim 4.8$ s marks the appearance of a $q_{min} = integer$ magnetic surface. Figure 7 shows that in the same JET discharge the ITB triggering event observed as an increase of T_e in the region close to ( ) R $q$min , happens at $t \sim 4.6$ s. This sequence of events is characteristic of the majority of similar JET discharges, where the ITB were triggered near integer q_{min} (t) in plasmas with non-monotonic q (r)-profiles. The ITB triggering event preceding the grand AC marking q_{min} $(t) = integer$ strongly indicates that the ITB triggering event is associated with the depletion in time of rational magnetic surfaces [11,12] just before min q reaches an integer value, rather than the presence of an integer min q value itself. Similar observations have been made on DIII-D [13]. The time correlation between ITB triggering events and Grand Cascades has been found to exist in JET plasmas with densities up to $\sim 5\times10^{19}$ m^{-3}, indicating that the timing of ITB triggering from ACs may facilitate ITB scenario development in machines with high densities (C-MOD, ITER).

4. NBI-DRIVEN ACS IN TRITIUM TRACE JET EXPERIMENT

Alfvén cascades driven by sub-Alfvénic NBI-produced ions, $V_{||NBI} \cong 0.2V_A$, have been detected for the first time using the O-mode interferometry on JET [5]. In this case, the ACs are best excited at lowest frequencies, which is determined by the geodesic acoustic effect upon the shear Alfvén continuum. This allows *super-sonic*, but sub-Alfvénic, NBI-produced ions to resonate with the ACs. A set of dedicated experiments has been performed recently on JET and DIII-D establishing the range of parameters $V_{||NBI}/V_A$ and P_{NBI} required for satisfying the resonant conditions and driving ACs [14]. Here, we point out that NBI-driven ACs were also observed during the JET tritium NBI blip experiments when the neutron rate was used for probing the T-beam transport. Figure 9 shows an example of power waveforms. It was found that even in the presence of ACs during the NBI T-blip the measured DT neutron profiles and total neutron yields agree well with the TRANSP code [15]. A good correlation is also found in this discharge between the calculated collisional transport and measured neutron yield temporal evolution, for both neutron measurements from DD and DT reactions, showing that the ACs had no significant effect on fast ion confinement in this case.

5. TRANSITIONS IN ALFVÉNIC SPECTRA DURING ITB FORMATION

Transitions from TAEs to ACs have been observed on JET when an ITB forms (Figure11). A temporal evolution of the current density profile consistent with the observed TAE-to-AC transition has been identified using Alfvén spectroscopy. It was found that this transition is caused by a reversal of the magnetic shear associated with the bootstrap current.

6. ALFVÉN GRAND-CASCADES ASSOCIATED WITH QMIN=1 IN SAWTOOTHING JET PLASMAS

Alfvén grand-cascades are usually used for diagnosing integer q_{min} >1 needed for developing ITB scenarios. A question arises whether the grand-cascades can be also caused by the presence of $q_{min} = 1$ magnetic surface. Such plasmas are strongly affected by the $q = 1$ sawteeth, which flatten current profile after each sawtooth crash However, some JET discharges with high T_e values and profiles of electron temperature strongly peaked within a very broad $q = 1$ radius do show the presence of ACs ($n = 1$ and $n = 2$) repeatedly occuring after each sawtooth crash as Figures 13 shows. In these discharges, ACs have also been used for diagnosing q_{min} in monster sawteeth in JET discharges with weakly reversed magnetic shear. From observations of the ACs and the EFIT reconstructed equilibrium, it was found with the MISHKA-1 [16] modelling of the ACs, that the crashes occur at min q ~0.85, whilst after the crashes $q_{min} > 1$ was deduced for this type of discharges [17].

7. THEORY DEVELOPMENT AND PROSPECTIVE APPLICATION OF ACS FOR DIAGNOSING KINETIC PLASMA PARAMETERS

It is likely that information about kinetic plasma parameters can be obtained from the lowfrequency properties of ACs, which were in the focus of recent theoretical development [18, 19]. A possibility

for diagnosing electron temperature T_e and/or the ratio of ion and electron temperatures, T_i/T_e, from observations of the lowest frequency of ACs, as well as fast ion density gradient follow from the low-frequency boundary of ACs in the form:

$$\left(f_{AC}^{Low}\right)^2 = \left(f_{AC}^{Geo}\right)^2 + \left(f_{AC}^{Hot}\right)^2 + \left(f_{AC}^{P}\right)^2, \tag{4}$$

where geodesic acoustic frequency deforming shear Alfvén continuum is given by

$$f_{AC}^{Geo} = \frac{1}{\pi\sqrt{2\, m_i R_0}} \left| T_e + \frac{7}{4} T_i \right|^{1/2}, \tag{5}$$

while the frequency offsets, f_{AC}^{Hot} and f_{AC}^{P}, are caused by the hot ion effect [20] and the plasma pressure gradients [19, 21], correspondingly. When the offset frequencies are negligibly small, one obtains from Eq.(5) the following relation:

$$T_e\,[eV] \bullet \left(1 + \frac{7}{4}\frac{T_i}{T_e}\right) \approx 3.77 \times (f_{AC}^{Low}\,[kHz])^2 \tag{6}$$

which may provide an estimate of T_e and T_i/T_e from detecting f_{AC}^{Low}. Estimate (6) was assessed in JET experiments and it was found, that such relation can only hold if the ICRH power accelerating fast ions driving ACs is low, $P_{ICRH} \leq 3$MW. For a higher value of ICRH power, the experimentally observed f_{AC}^{Low} becomes higher than that given by Eq.(6). Estimate of f_{AC}^{Hot} and f_{AC}^{P} has shown that the offset f_{AC}^{Hot} is the most likely cause, that invalidates the assumption $|f_{AC}^{Hot}| << f_{AC}^{Geo}$.

SUMMARY

A systematic study of interferometry and reflectometry techniques detecting AEs via electron density perturbations has been successfully performed on JET. It was demonstrated that O-mode and far infrared interferometry techniques, as well as X-mode reflectometry can be used for AE density perturbation measurements. The interferometry technique of detecting ACs provided the AC observations with high time resolution, and it was found that ITB triggering events precede grand cascades. This suggests that the spontaneous improvement of plasma confinement is associated with the effect of rational depletion just before $q_{min}(t)$= *integer* times, rather than with the presence of the integer magnetic surfaces in the plasma. The correlation between grand-ACs and ITB triggering events was found to persist up to densities 5×10^{19} m^{-3} in JET discharges. NBI-driven ACs in JET discharges with tritium NBI blips were found to have at most a small effect on fast particle confinement as the measured DT neutron profiles and total neutron yields agree well with the TRANSP code modelling based on Coulomb collisions. Transitions from TAEs to ACs observed in some JET discharges were explained by the shear reversal triggered by ITB and associated increased bootstrap current. grand-cascades observed in JET plasmas with monster sawteeth and broad q=1 radius allowed investigation of sawtooth crashes in such discharges. It was found that sawtooth crashes occur at $q_{min}(t)$ ~0.85, while $q_{min}(t)$ >1 condition

has been deduced for after-crash phase. This paper also suggests a plasma temperature diagnostics via Alfvén spectroscopy employing the low-frequency part of the ACs. Preliminary analysis exploring this diagnostic is encouraging and further development will follow to assess its actual capabilities. The Alfvén spectroscopy is shown to be a robust and useful tool in analysing some important features of JET discharges.

ACKNOWLEDGEMENTS

This work was partly supported by the UK Engineering and Physical Sciences Research Council, and by the European Communities under the contract of Association between EURATOM and UKAEA. The views and opinions expressed herein do not necessarily reflect those of the European Commission. This work was partly conducted under the European Fusion Development Agreement.

REFERENCES

[1]. GOELDBLOED J.P. et al., Plasma Physics Controlled Fusion **35** (1993) B277
[2]. SHARAPOV S.E. et al., Phys. Letters **A289** (2001) 127
[3]. FASOLI A. et al., Plasma Physics Control. Fusion **44** (2002) B159
[4]. NAZIKIAN R., et al., Phys. Rev. Lett. **91** (2003) 125003
[5]. SHARAPOV S.E. et al., Phys. Rev. Lett. **93** (2004) 165001
[6]. HACQUIN S. et al., Nucl. Fusion **46** (2006) S714
[7]. ALPER B. et al., 47th Annual Meeting of APS DPP, Denver, USA (2005)
[8]. HACQUIN S. et al., 33rd EPS Conference on Plasma Phys. Control. Fusion, Rome, 19-23 June (2006)
[9]. SHARAPOV S.E. et al., Nuclear Fusion **46** (2006) S868
[10]. JOFFRIN E. et al., Nucl. Fusion **43** (2003) 1167
[11]. BEKLEMISHEV A.D. and HORTON W., Phys. Fluids B4 (1992) 200
[12]. GARBET X. et al., Nucl. Fusion **43** (2003) 975
[13]. AUSTIN M.E. et al., Physics of Plasmas **13** (2006) 082502
[14]. BORBA D. et al., 21st IAEA Fusion Energy Conference, post-deadline paper (2006)
[15]. BUDNY R. et al., Nuclear Fusion **32** (1992) 429
[16]. MIKHAILOVSKII A.B. et al., Plasma Phys. Reports **23** (1997) 844
[17]. SANDQUIST P., Alfvén Eigenmodes, Sawtooth Oscillations and Fast Ion Confinement in Alpha-Simulation JET Experiments, Ms. Thesis, Chalmers University, Gothenburg (2004)
[18]. BREIZMAN B.N. et al., Physics of Plasmas **12** (2005) 112506
[19]. FU G.Y. and BERK H.L. Physics of Plasmas **13** (2006) 052502
[20]. BERK H.L. et al., Phys. Rev. Lett. **87** (2001) 185002
[21]. KRAMER G.J. et al., Physics of Plasmas **13** (2006) 056104
[22]. BREIZMAN B.N. in: Theory of Fusion Plasmas, Proceed. of Varenna-Lausanne Workshop (2006) (to be published)

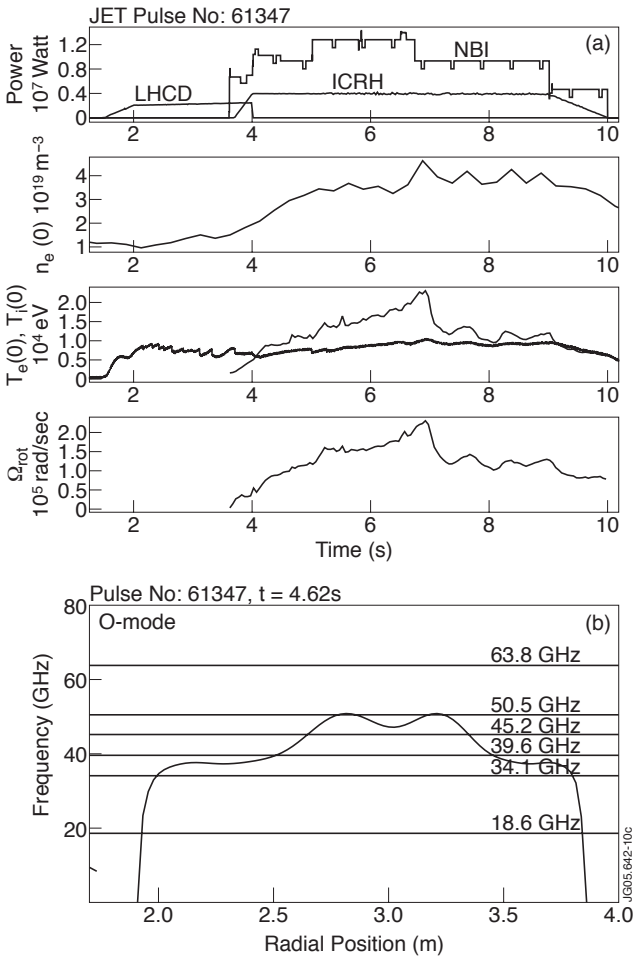

Figure 1: (top) Time evolution of ICRH, NBI, and LHCD power, electron density, electron and ion temperatures, and toroidal plasma rotation in JET pulse No: 61347; and (bottom) O-mode interferometer: the frequencies of microwave beams and O-mode cut-off profile are shown.

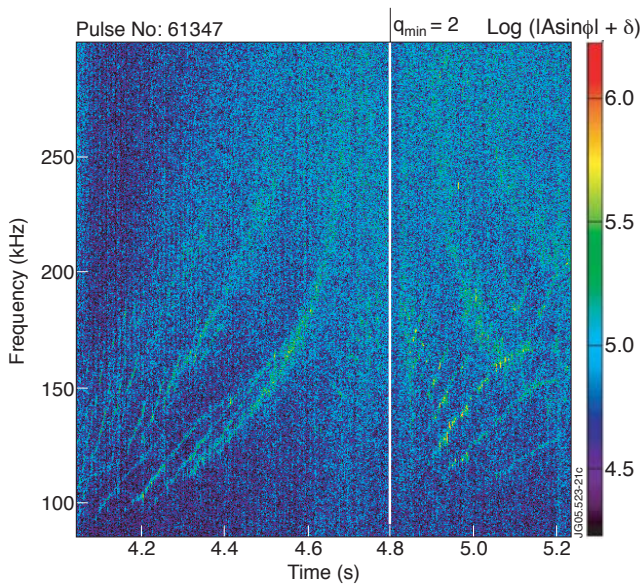

Figure 2: ACs detected with the O-mode interferometry in JET Pulse no: 61347. Microwave beam frequency of 63.8GHz is above the cut-off frequency ~50GHz as Fig.1 (bottom) shows. These ACs are not seen on Mirnov coils. A grand cascade occurs at t ~ 4.8s

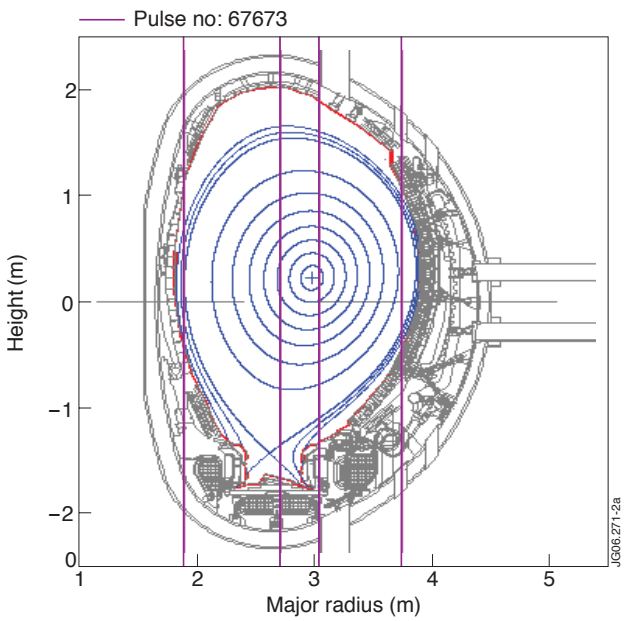

Figure 3: Geometry of JET interferometer with vertical lines-of-sights (counted from left to right as Channels 1,..,4)

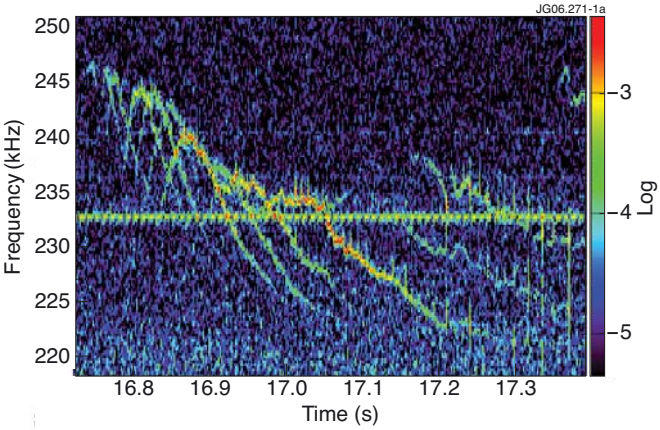

Figure 4: Tornado modes (TAEs inside the q=1 magnetic surface) detected with vertical Channel 3 of the JET interferometer (passing through the magnetic axis).

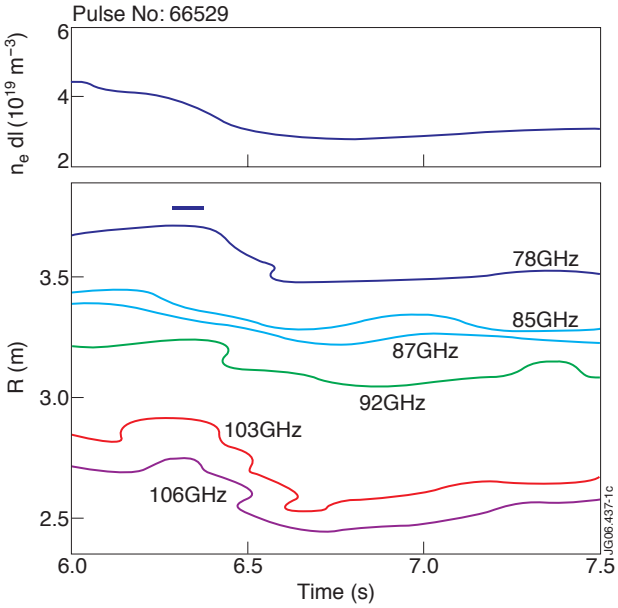

Figure 5: (top) Evolution of equilibrium lineintegrated plasma density; (bottom) Evolution of the cut-off layers for different frequency microwave beams

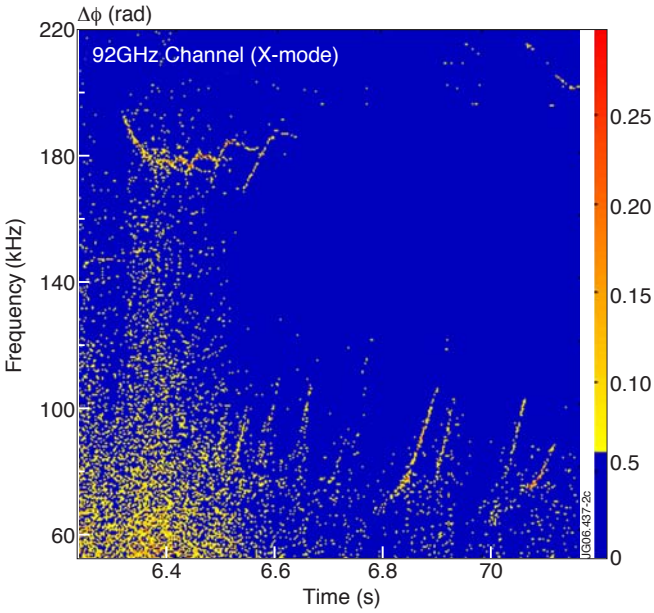

Figure 6: Alfvén Cascades are seen at frequencies from 60kHz to 120kHz, and TAEs are seen at 180–200kHz with X-mode reflectometry probing wave of frequency 92GHz.

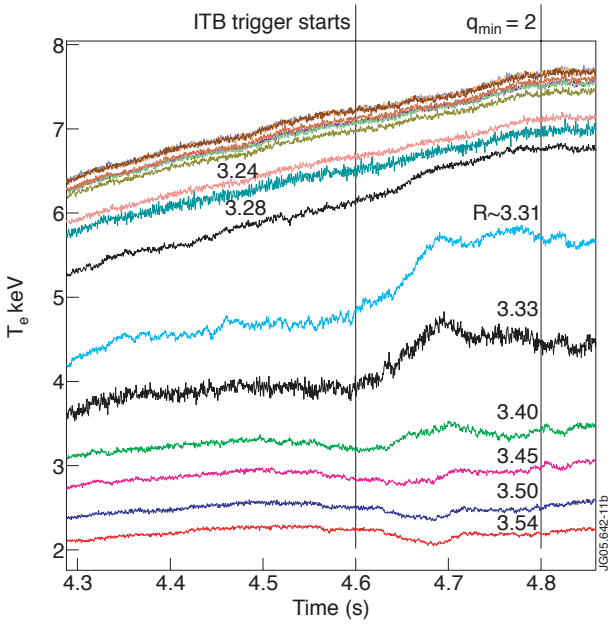

Figure 7: Electron temperature traces measured with multi-channel ECE in JET discharge #61347. An ITB triggering event is seen at t ~ 4.6s

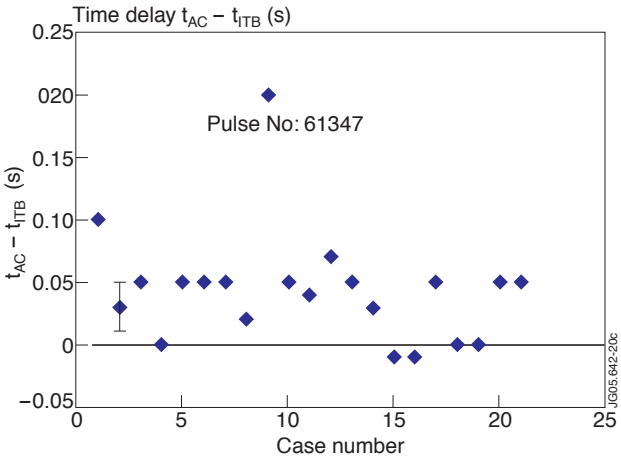

Figure 8: Time delay between grand ACs and ITB triggering events for a set of discharges with interferometry diagnostic used for AC detection.

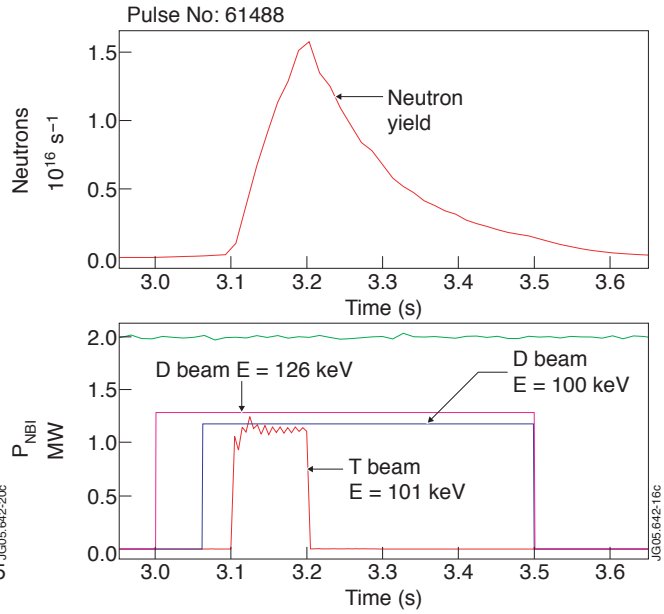

Figure 9: Tritium NBI-blip experiment: time evolution of neutron yield R_{nt} and NBI power from D and T NBI sources in JET Pulse No: 61488: B_T =3.45 T, $I_P \leq$ 2 MA.

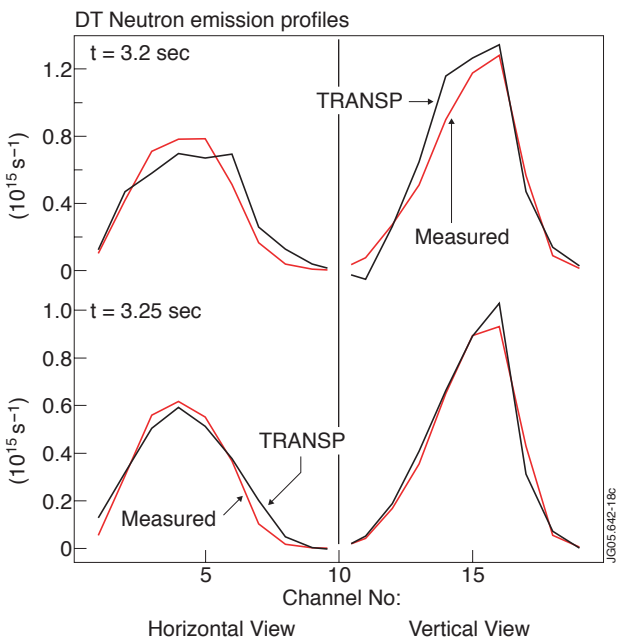

Figure 10: TRANSP modelling versus DT neutron profiles for Pulse No: 61488. Channels 1-10 show the horizontal view neutron camera measurements (from top ch.1 to bottom ch.10), channels 11-19 show the vertical view neutron camera measurements (from HFS ch.11 to LFS ch.19).

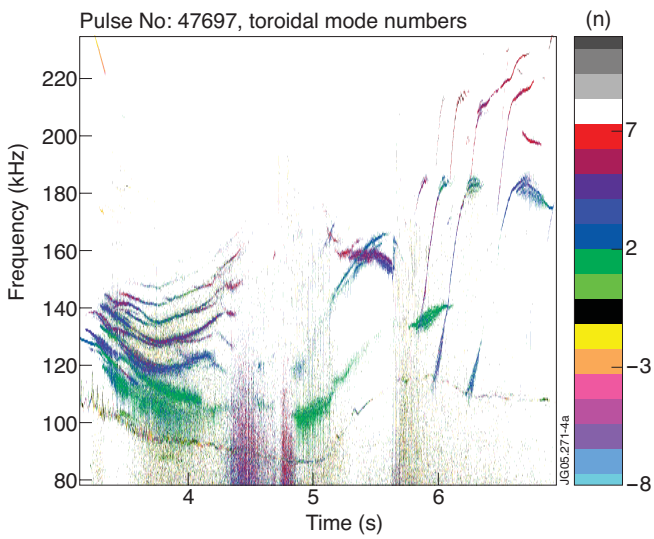

Figure 11: Transition from TAE dominated Alfvén spectrum to AC spectrum. The ITB forms at t=4.6s.

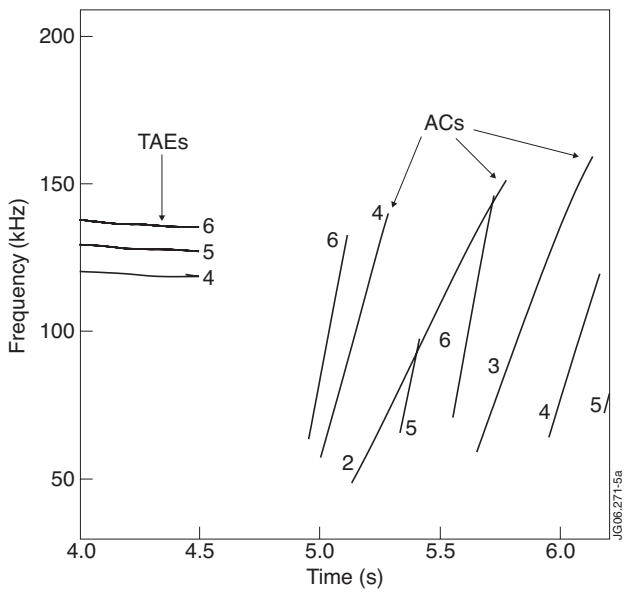

Figure 12: Incompressible MISHKA-1 code [16] shows that ACs only appear after 4.9s in the model with growing amplitude bootstrap current.

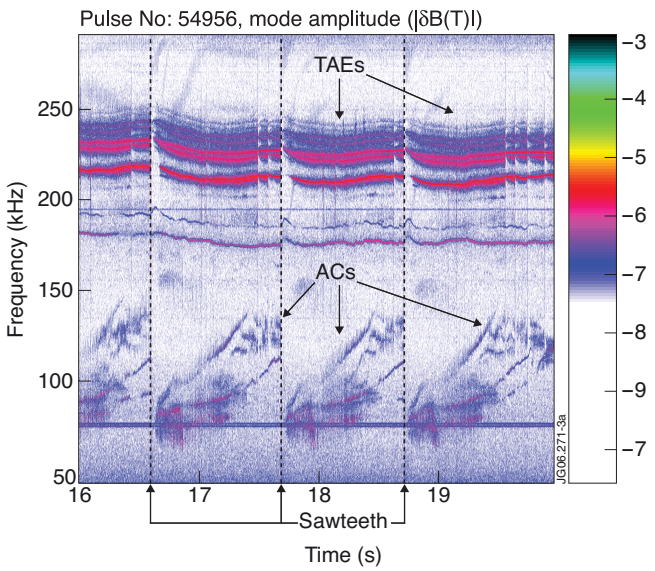

Figure 13: ACs and TAEs in JET Pulse No: 54956 with monstersawteeth.